ApoStream™, a new dielectrophoretic device for antibody independent isolation and recovery of viable cancer cells from blood

Vishal Gupta,[1] Insiya Jafferji,[1] Miguel Garza,[1] Vladislava O. Melnikova,[1] David K. Hasegawa,[1] Ronald Pethig,[2] and Darren W. Davis[1,a)]

[1]*ApoCell, Inc., Houston, Texas 77054, USA*
[2]*Institute for Integrated Micro and Nano Systems, School of Engineering, University of Edinburgh, Edinburgh EH9 3JF, United Kingdom*

Isolation and enumeration of circulating tumor cells (CTCs) are used to monitor metastatic disease progression and guide cancer therapy. However, currently available technologies are limited to cells expressing specific cell surface markers, such as epithelial cell adhesion molecule (EpCAM) or have limited specificity because they are based on cell size alone. We developed a device, ApoStream™ that overcomes these limitations by exploiting differences in the biophysical characteristics between cancer cells and normal, healthy blood cells to capture CTCs using dielectrophoretic technology in a microfluidic flow chamber. Further, the system overcomes throughput limitations by operating in continuous mode for efficient isolation and enrichment of CTCs from blood. The performance of the device was optimized using a design of experiment approach for key operating parameters such as frequency, voltage and flow rates, and buffer formulations. Cell spiking studies were conducted using SKOV3 or MDA-MB-231 cell lines that have a high and low expression level of EpCAM, respectively, to demonstrate linearity and precision of recovery independent of EpCAM receptor levels. The average recovery of SKOV3 and MDA-MB-231 cancer cells spiked into approximately 12×10^6 peripheral blood mononuclear cells obtained from 7.5 ml normal human donor blood was 75.4% ± 3.1% (n = 12) and 71.2% ± 1.6% (n = 6), respectively. The intra-day and inter-day precision coefficients of variation of the device were both less than 3%. Linear regression analysis yielded a correlation coefficient (R^2) of more than 0.99 for a spiking range of 4–2600 cells. The viability of MDA-MB-231 cancer cells captured with ApoStream was greater than 97.1% and there was no difference in cell growth up to 7 days in culture compared to controls. The ApoStream device demonstrated high precision and linearity of recovery of viable cancer cells independent of their EpCAM expression level. Isolation and enrichment of viable cancer cells from ApoStream enables molecular characterization of CTCs from a wide range of cancer types. © *2012 American Institute of Physics.*
[http://dx.doi.org/10.1063/1.4731647]

I. INTRODUCTION

Among the characteristic rate-limiting steps of metastatic cancer progression is vascular dissemination of tumor cells.[1] Normally absent from the peripheral blood of healthy donor, circulating tumor cells (CTCs) are increasingly used as biomarkers from patients with metastatic cancer.[2,3] CTC counts correlate negatively with progression free survival and overall survival in patients with metastatic colorectal, breast, and prostate cancer.[3–8] Growing evidence

---

a)Author to whom correspondence should be addressed. Tel.: +01 (713)-440-6070. Fax: +01 (713)-440-6074. Electronic mail: ddavis@apocell.com.

suggests that CTC isolation from a blood sample may allow reliable early detection and molecular characterization of cancer at diagnosis and may provide a minimally invasive method to guide and monitor the results of cancer therapy. For example, the presence of epidermal growth factor receptor (EGFR) mutations in circulating lung cancer cells has been shown to correlate with reduced progression free survival.[7] In addition, monitoring the response of circulating breast cancer cells to adjuvant chemotherapy allowed detection of patients at risk of early relapse.[9,10]

CTCs are rare cells present in the blood in numbers as low as one CTC per 10^6-10^7 leukocytes, which makes their capture and detection very challenging. The techniques currently used for CTC capture include immunomagnetic separation,[6,8] membrane filters,[11,12] and micro-electro-mechanical system (MEMS) chips.[13,14] All of these techniques are subject to limitations.[15] For example, immunomagnetic separation relies on the expression of known cell surface markers such as the epithelial cell adhesion molecule (EpCAM) and hence is restricted to a few epithelial cancers with high EpCAM expression. CTC enumeration by CellSearch® is a Food and Drug Administration (FDA) cleared biomarker test that utilizes EpCAM for CTC capture, but indications are limited to metastatic colorectal, breast, and prostate cancer.[3,16] It is inapplicable to cancers of non-epithelial origin such as melanoma, brain cancers, and sarcomas as well as advanced metastatic disease where EpCAM expression is lost.[17,18]

The immunomagnetic isolation procedure associated with CTC identification with the CellSearch system involves chemical and mechanical manipulation that creates challenges to culture these cells for downstream analysis. While isolation of rare cells in a viable state may facilitate research into the molecular underpinnings of cancer progression and enable more accurate planning of personalized therapy, it remains technologically challenging and is thus underutilized in the medical community. Development of novel, robust technologies for rare cell isolation which create the opportunity to conduct post processing studies on viable cells will be an important advancement toward understanding the biology and clinical applications of rare cells.

Prior studies have successfully demonstrated the ability of dielectrophoretic field-flow fractionation (DEP-FFF) technology to characterize and capture cancer cells from peripheral blood mononuclear cells (PBMCs).[19,20] In these earlier studies, DEP-FFF was applied using a batch mode configuration that limited the number of cells processed in a given run because cells must remain spaced by several diameters to avoid dipole–dipole interactions that can perturb DEP responses.[19,21] As a result, the loading capacity using the batch mode of operation was limited to less than a million cells per run and required processing of multiple batches in order to complete a CTC analysis for a typical 7.5 ml blood sample.

Other recent studies reported the use of various types of DEP micro devices for cancer cell isolation in preclinical models. For example, DEP has been used to separate colorectal cancer cell lines in a microfluidic chip.[22] Contactless DEP microfluidic device was utilized to study the behavior of mouse ovarian cells.[23] Human cervical carcinoma cell line HeLa was concentrated using circular microelectrodes.[24] DEP-based printed circuit boards have been used for software controlled entrapment and movement of human tumor cells.[25] Oral squamous cell carcinoma cells[26] and mouse melanoma clones[27] have been isolated using DEP technology. Human breast cancer cells have been isolated using a multi-orifice flow fractionation DEP device,[28] a DEP-activated cell sorter,[29] and a DC-DEP device.[30] All these devices, with the exception of the device described in this study, have low throughput which limits their clinical utility as devices for rare cell isolation from blood.

To overcome the cell throughput limitations of the DEP batch mode configuration to allow for the efficient isolation and enrichment of CTCs from whole blood, we developed the continuous flow ApoStream™ device. Herein, we describe the operational optimization and performance characteristics of ApoStream, to capture cancer cells independent of antigen expression levels such as EpCAM. The ApoStream technology has the advantage of antibody independent separation of viable cancer cells enabling CTC capture from a wide variety of cancer types allowing multiple downstream processes and cell culture expansion.

II. THEORY AND DEVICE SETUP

There have been extensive publications on the dielectric properties of dissimilar cells and DEP-based methods for isolating cells.[31–34] Many studies have utilized DEP-FFF methods that exploit the balance of DEP forces, sedimentation forces, and hydrodynamic lift forces to position cells in a hydrodynamic flow profile.[19,35–38] The ApoStream device uses DEP to sort cells with distinct biophysical characteristics by exploiting dissimilarities in the frequency-dependent dielectric properties of different cell types that arise from morphologic and electrical conductivity differences.[21] The isolation of rare cancer cells from blood in particular exploits differences in dielectric properties between blood cells (lymphocytes, monocytes, and granulocytes) and cancer cells.[19,20] For the separation of cancer cells from healthy blood cells, the ApoStream device operates in a modified form to conventional DEP-FFF, in that the cancer cells are attracted by positive DEP forces towards the electrode plane, and thus away from the bulk of the blood cells that are levitated by negative DEP into the hydrodynamic flow velocity profile. This is accomplished by applying the voltage signal at a frequency in between the so-called DEP crossover frequency of cancer cells and PBMCs. The crossover frequency is defined as the frequency where the DEP force makes the transition from a negative to a positive force and is dependent on cell and medium conductivity and permittivity.[19,21] The mean crossover frequencies of breast, lung, and ovarian cancer cell lines were reported to be low (30-40 kHz) compared to 90-140 kHz for major peripheral blood cell types at 30 mS/m eluate buffer conductivity.[19,20] This difference in crossover frequencies forms the basis for isolation of CTCs from a complex mixture of cells and is applicable to a wide variety of cancer types. When a frequency in the range of 45-85 kHz is applied, the cancer cells experience positive (attractive) DEP force, while the blood cells are repelled into the fluid flow with negative DEP force, resulting in separation.[19]

The DEP force (F_{DEP}) acting on a spherical cell of radius r, suspended in a liquid medium of absolute permittivity ε_s, is given by the relationship[39,40]

$$F_{DEP} = 2\pi\varepsilon_s r^3 \mathrm{Re}(f_{CM})\nabla E^2 \qquad (1)$$

where E is the RMS value of the applied electric field and ∇ is the gradient operator. $\mathrm{Re}(f_{CM})$ is the real part of the Clausius-Mossotti factor that defines the effective polarizability of the cell relative to that of the suspending medium.[40] Amongst several simplifying assumptions, a relevant one for our present studies is that the electric field in the vicinity of the cell is not perturbed by the presence of a boundary, such as a metal or dielectric surface.[21] From the studies of Lo and Lei,[41] the ratio of the electrode boundary perturbing force to the DEP force is of the order $(L/h)(r/2h)^3$, where h is the height above the electrode plane and L is the length scale of the electric field. For the interdigitated, parallel electrodes used in the ApoStream device, L can be taken to be the distance of 50 μm between opposing electrodes.[21] For a cell of radius 5 μm located with its centre 15 μm above the electrode surface, the boundary perturbation would represent only 1.6% of the primary DEP force and does not substantially influence the validity of Eq. (1). The perturbing influence of the electrode and inter-electrode surfaces increases rapidly as the levitation height falls below this level and becomes particularly dependent on the electrode geometry and cell diameter.[42]

Equation (1) can be modified[36,43] to describe the vertical component of the DEP force averaged along a horizontal plane, acting on a cell at height h above the electrode plane, to the form

$$F_{DEP}(h) = 2\pi\varepsilon_s r^3 p(f)\mathrm{Re}(f_{CM})q(h)V^2. \qquad (2)$$

The factor p(f) defines the frequency dependent electrode polarization which becomes an important factor at low frequencies, V is the applied RMS voltage, and q(h) reflects the height dependence of the vertical DEP force component, which above a certain levitation height can be taken to decrease smoothly as a function of increasing levitation height. However, at low levitation heights, there is a sharp departure from the form of Eq. (2), the details of which depend on

the electrode geometry.[43] Local values of the vertical component of the DEP force are determined by the factor ∇E^2 in Eq. (1), with sharp maxima occurring above electrode edges.[44] A theoretical analysis of the Stokes drag force acting on a particle brought down by positive DEP towards the electrode plane in a continuous flow DEP chamber requires correction for ill-defined wall effects, and at these heights, there is no linear relation between V^2 and the fluid flow rate to give the levitation produced by negative DEP.[44] These facts preclude a detailed theoretical study of the operating parameters for our device, and optimization of its performance was performed by a simple design-of-experiment procedure.

The complete setup of the continuous flow ApoStream device is shown in Figure 1. The gear pump, custom-made DEP signal generator, conductivity meter, and laser particle counter are computer controlled allowing dynamic feedback control and monitoring. The sample injection and collection flow rates are controlled by high precision syringe pumps. The captured cancer cells are collected into a microcentrifuge tube.

The ApoStream flow chamber applies an AC electric field to the sample within a defined region of the flow path. A flexible polyimide film sheet with electroplated copper and gold electrodes forms the floor of the flow chamber, an acrylic sheet forms the ceiling of the flow chamber, and a gasket forms the side walls of the chamber. Eluate buffer is introduced at the upstream end of the flow chamber. The sample is introduced through a rectangular port located in the floor of the flow chamber at the upstream end. Cancer cells are collected through another rectangular port located downstream from the sample inlet port (Figure 1). The sample is injected at a low flow rate into the bottom of the flow chamber to minimize cell levitation and to ensure cells stay within the effective DEP field. When cells encounter the DEP field, the DEP forces pull cancer cells towards the chamber floor and repel other cells as they traverse
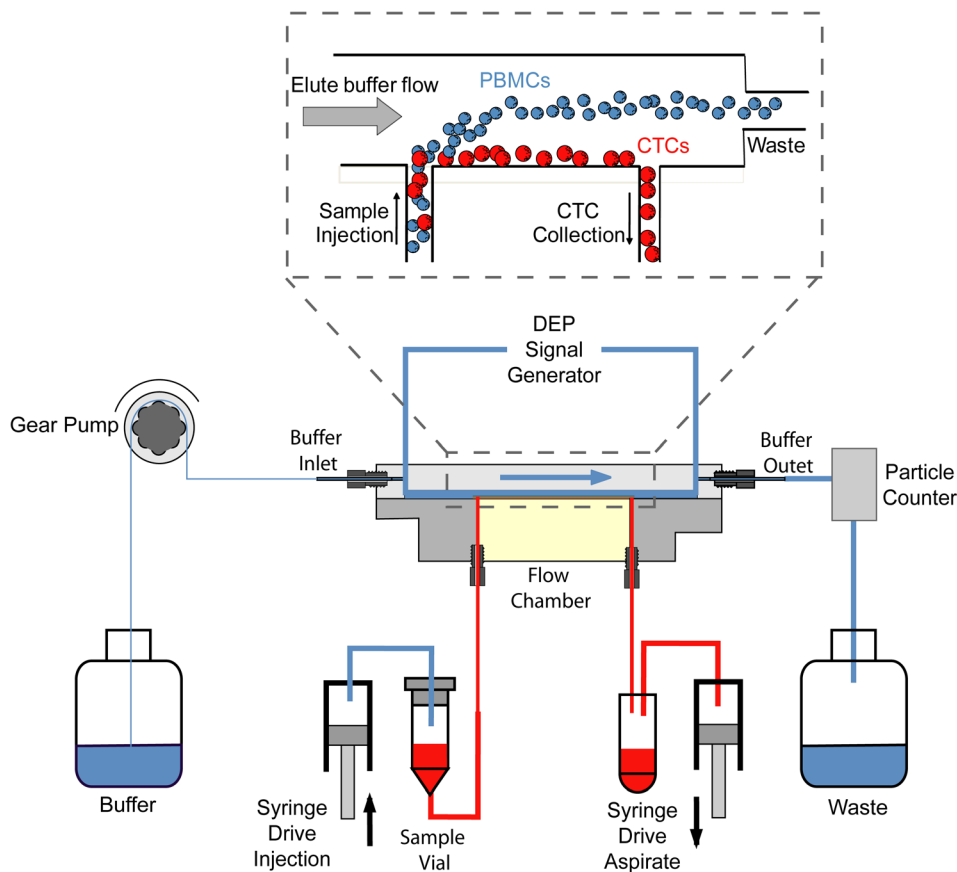
FIG. 1. Schematic diagram of the ApoStream device; inset shows cell flow and separation in the flow chamber. (For details, see explanation in the text).

the electrode. As shown in Figure 1 (inset), cancer cells travelling close to the chamber floor are withdrawn through the collection port, while other blood cells traveling at greater heights are carried beyond this port and exit the chamber to the waste container via a second outlet port.

III. MATERIALS AND METHODS

A. Cancer cell isolation using ApoStream

The following describes the procedure used for the operation of the ApoStream device to isolate cancer cells for the performance characterization studies.

Prior to initiating each run, the ApoStream flow chamber was disinfected with 70% ethanol followed by preconditioning with sucrose based eluate buffer with a conductivity of 30 mS/m. The low surface tension of the ethanol solution, compared to water, also aided the avoidance or removal of air bubbles. Samples were prepared by isolating PBMCs from 7.5 ml of whole blood using a standard Ficoll density gradient method. PBMCs were spiked with pre-stained cancer cells in 1 ml of the optimized sample buffer. The cell suspension was loaded in the custom sample injection vessel as shown in Figure 1. The sample was injected through the chamber floor using a syringe pump. A gear pump was used to deliver eluate buffer continuously at a constant flow rate. An AC voltage (2-4.5 Vp-p) was applied to the electrode to initiate the DEP field. Cancer cells were collected through the collection port at 18-25 μl/min flow rate into a microcentrifuge tube. The total run time to process each PBMC sample preparation through ApoStream was approximately 60 min. After each run, the flow chamber was cleaned with Terg-a-zyme® (Alconox, White Plains, NY) detergent solution. The protease enzyme in Terg-a-zyme® breaks down the cell membrane to eliminate cell carryover.

The locations of the sample injection and sample collection ports with respect to overall flow chamber dimensions are shown in Figure 2(a). Videos were captured to demonstrate cancer cell isolation from PBMCs using ApoStream as shown in Figures 2(b) and 2(c). In these videos, SKOV3 cancer cells and PBMCs were pre-stained with green fluorescent CellTracker™ dye (staining procedure described below) and run through the ApoStream device in independent experiments. The videos were taken using an Olympus SZX16 fluorescence microscope (Olympus Corporation, Japan) positioned above the flow chamber over the cell collection port. A portion of the interdigitated electrode, viewable as a series of light, parallel stripes, is visible in the Figures 2(b) and 2(c).

B. Cell culture and spiking studies

Cancer cell lines SKOV3 (ovarian cancer) and MDA-MB-231 (breast cancer) were purchased from American Type Culture Collection (ATCC, Manassas, VA). SKOV3 and MDA-MB-231 cells were cultured in McCoys 5 A medium (Lonza, Walkersville, MD) and DMEM medium (Lonza), respectively, and supplemented with 10% fetal bovine serum and 1% penicillin/streptomycin.

For the spiking studies, cancer cells were pre-stained with CellTracker™ (Invitrogen, Eugene, OR) dye to allow for post ApoStream enrichment enumeration. Dye stock solution (~10 mM) was prepared by adding 11 μl of sterile dimethyl sulfoxide (DMSO) to 50 μg of dye powder. Five (5) μl of the dye stock solution was added to the cell suspension (~500 000 cells/ml) and the cells were incubated for 30 min at 37 °C followed by centrifugation at 1000 g for 3 min. The cells were then washed twice with 1 ml of sterile culture medium and left in the culture medium until spiked into PBMCs from normal donor blood.

Blood was collected from healthy human donors in BD Vacutainer® tubes (BD, Franklin Lakes, NJ). PBMCs were isolated from 7.5 ml of blood using manufacturers' standard density gradient methods (GE Healthcare, Uppsala, Sweden; BD, Franklin Lakes, NJ). PBMCs were resuspended in 1 ml of ApoStream sample buffer prior to further use.

Pre-stained cancer cells were spiked into PBMCs and separation was performed using the ApoStream device. To determine mean spiking count, the same spiking volumes were pipetted onto microscope slides in triplicate. Cells were manually counted using an Olympus BX41
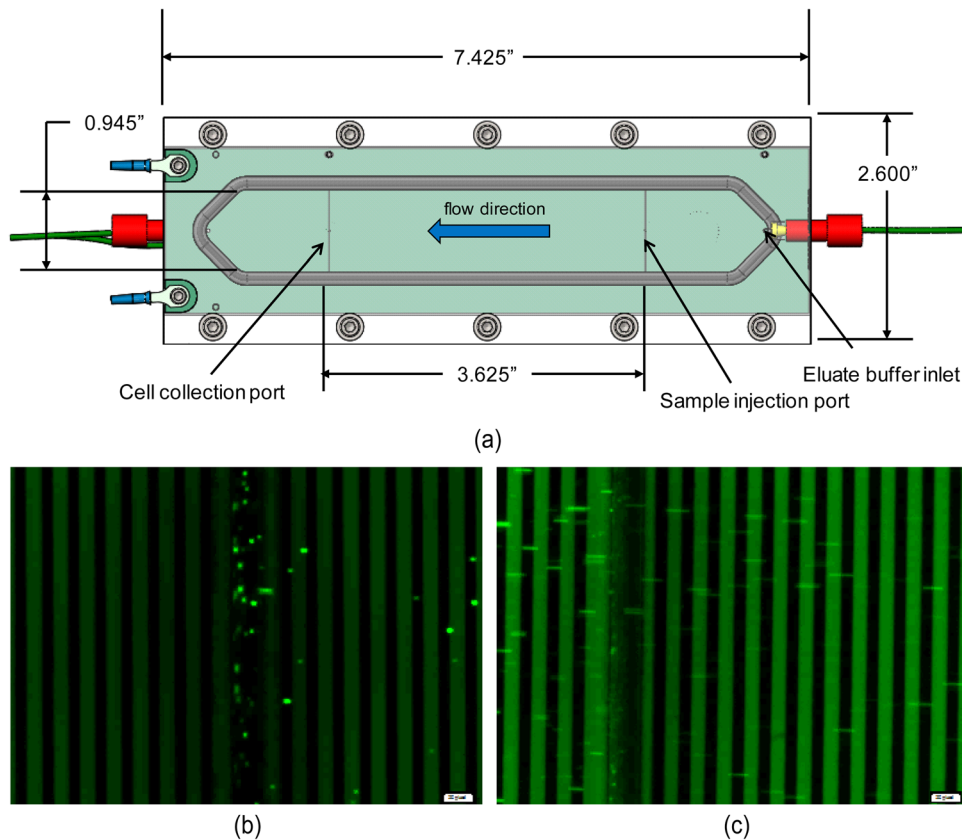
FIG. 2. (a) Schematic of the top view of the flow chamber showing sample injection and sample collection port locations. (b) Still image from video demonstrating the flow and collection of fluorescently labeled SKOV3 cancer cells through the collection port in the ApoStream flow chamber. Cancer cells are collected into the collection port when the DEP field is activated. (c) Still image from video demonstrating the flow of fluorescently labeled PBMCs through ApoStream flow chamber. The first half of the video (∼10 s) demonstrates that most PBMCs fall into the collection port when the DEP field is not active. The second half of the video (from 11 to 21 s) demonstrates that upon the activation of DEP field the PBMCs are repelled from the electrode causing them to move into the high velocity flow region and are no longer being pulled into the collection port (enhanced online) [URL: http://dx.doi.org/10.1063/1.4731647.1] [URL: http://dx.doi.org/10.1063/1.4731647.2].

fluorescence microscope. Counts of cancer cells enriched with the ApoStream device were divided by the mean spiked cell count to determine cell recovery efficiency.

C. Device parameter optimization

The performance of the ApoStream device was optimized in two series of experiments. First, the eluate buffer, sample injection, and sample collection flow rates were optimized to maximize cancer cell recovery while minimizing PBMC contamination. Second, a 2-level 3 parameter factorial design of experiment (DOE) using DESIGN EXPERT 8 software (Stat-Ease, Minneapolis, MN) was utilized to optimize frequency, voltage, and the sample collection rate. A response surface methodology (RSM) was utilized to demonstrate the cells' response (recovery performance) to frequency and sample injection rate. SKOV3 cancer cells lines and normal donor PBMCs were used in independent experiments to optimize the separation parameters and subsequently, the SKOV3 cells were spiked into PBMCs to assess performance with those optimized parameters.

D. Buffer optimization

Following the selection of optimum device parameters, experiments were conducted to optimize eluate and sample buffer formulations to maintain cell viability and reduce cell loss.

A sucrose-based buffer was used as the eluate and a mix of RPMI growth medium with additives was used as the sample buffer. The eluate buffer composition included 9.5% sucrose (Sigma-Aldrich, St. Louis, MO), 0.01% dextrose (Fisher, Hanover, IL), and 1 mM phosphate buffer *p*H 7.0 to maintain the cell osmolarity under physiological conditions.[19,20] The eluate buffer conductivity was adjusted to 30 mS/m using sodium chloride (Sigma-Aldrich). The sample buffer, used to resuspend the cell mixture, contains RPMI cell culture growth medium. The eluate and the sample buffer formulations were optimized by adding bovine serum albumin (BSA, Sigma-Aldrich) as a nutrient and to minimize cell adherence to surfaces, Pluronic F-68 (Sigma-Aldrich) for cell membrane stability, an anti-oxidant compound as free radical scavenger and catalase (Sigma-Aldrich) to decompose hydrogen peroxide.

The sucrose concentration in the eluate buffer affects the osmolarity of the fluid. At a concentration of 9.5%, the eluate buffer osmolarity is 320 mOs/l. A reduction in the sucrose concentration could be beneficial in downstream analytical processing steps and it has been shown that osmolarity as low as 120 mOs/l does not significantly alter the dielectric properties of the cancer cells.[20] Therefore, the sucrose concentration was included as a variable in the buffer optimization study.

To determine optimum eluate and sample buffer formulations, a 2-level, 3 factor DOE spiking study was performed. The 3 factors were osmolarity (100 and 320 mOs/l; adjusted by changing sucrose concentration); eluate buffer (with and without additives); and sample buffer (with and without additives). In each of the conditions tested, approximately 5000 SKOV3 cells were spiked into PBMCs obtained from 4 ml of normal human donor blood. Enumeration of cells recovered after ApoStream™ separation was compared to determine the optimum formulations.

E. Device performance characterization

To demonstrate the performance of the ApoStream device, intra-day, inter-day, inter-device, and inter-operator precision, and linearity were determined for cancer cell recovery. Clinical and Laboratory Standards Institute (CLSI) guidelines EP5-2 A and EP06-A were utilized analyze the precision and linearity, respectively. Precision studies were run with PBMCs isolated from 7.5 ml of normal healthy donor blood that were spiked with either approximately 5000 SKOV3 cells or approximately 500 MDA-MB-231 cells. The spiked samples were processed through different ApoStream devices and flow chambers by multiple operators on multiple days. To demonstrate linearity, a series of experiments were conducted by spiking varying amounts of SKOV3 and MDA-MB-231 cells (ranging from 4 to 2600 cells) into PBMCs obtained from healthy donors.

F. Cell viability studies

MDA-MB-231 cancer cells were used to assess the viability and propagation of cells in tissue culture after isolation from ApoStream in independent experiments. Approximately 100 000 cancer cells were spiked into buffer and processed through the ApoStream device at physiological buffer osmolarity of 320 mOs/l. The collected cells were counted immediately after isolation and plated in 96-well plates ($\sim$1000 cells/well in triplicate for each time point) to test their growth potential. The cells in 96-well plates were incubated at 37 °C with 5% CO_2 for up to 7 days. The cells were harvested using trypsin at time points of 1, 2, 3, 5, and 7 days and viability was determined using the trypan blue exclusion method. Cell adherence to tissue culture plastic surface and propagation were also assessed by examining the cell culture well at each time point with an inverted microscope. Control cells that were not subject to ApoStream separation were also cultured for comparison.

IV. RESULTS AND DISCUSSION

A. Cancer cell isolation using ApoStream

The flow and collection of cancer cells and PBMCs through the collection port in the ApoStream flow chamber was demonstrated in the videos in Figures 2(b) and 2(c). In these videos,

the microscope is positioned above the flow chamber over the cell collection port. The video in Figure 2(b) demonstrates the flow and collection of cancer cells under an active DEP field. Cancer cells experience a positive DEP force at an applied frequency greater than the crossover frequency of cancer cells and are drawn to the chamber floor where the flow velocity is lower enabling capture via the collection port. The video in Figure 2(c) shows the flow of PBMCs through the ApoStream flow chamber. The first half of the video (~10 s) demonstrates that most PBMCs are pulled into the collection port due to the skimming action generated by the collection pump when the DEP field is not active. The sample is injected close to the chamber floor under laminar flow conditions to minimize mixing thereby maintaining all cells in the low velocity profile region near the bottom of the chamber. The second half of the video (from 11 to 21 s) demonstrates that upon the activation of DEP field, the PBMCs are repelled from the electrode causing the cells to move into the high velocity flow region and are no longer being collected in the collection port. These videos demonstrate DEP forces can be used to effectively separate cancer cells from PBMCs in ApoStream's laminar flow microfluidic chamber.

The ApoStream device takes 60 min to process approximately 12×10^6 PBMCs (suspended in 1 ml of sample buffer) from 7.5 ml of whole blood. The throughput of the ApoStream device is faster as compared to other small microfluidic chip based DEP technologies.[19,22,32,45] A study by Hu *et al.* showed a higher throughput of 10 000 cells per second, which is almost the twice the throughput of ApoStream device. However, that technology was limited to cell labeling.[46] The ApoStream device throughput can be further increased by enhancing the flow channel area and increasing the sample injection rate.

B. Device parameter optimization

There are a number of operating parameters which potentially affect ApoStream device performance. The eluate, sample injection, and collection flow rates are inter-dependent variables and were balanced to optimize cancer cell levitation, cancer cell skimming, and throughput (processing time). Also, because prior studies indicated that the DEP field effectiveness diminishes significantly at distances greater than approximately 30 μm from the electrode surface,[36,47] flow rates were selected to limit cell levitation to ~30 μm above the chamber floor. In addition, testing of varying eluate flow rates revealed lower cell collection performance with higher eluate flow rates (data not shown). These results suggest that the hydrodynamic lift forces begin to dominate with an increase in eluate flow rate, and that the cells are driven away from the chamber floor preventing them from being collected through the collection port located in the floor of the flow chamber. An increase in the applied voltage from 2 Vp-p to 4 Vp-p significantly decreased the PBMC contamination but did not have a significant effect on cancer cell collection (data not shown). At higher applied voltages, the electric field gradients are larger resulting in stronger DEP forces as these forces are proportional to the square of field gradient as described in Eqs. (1) and (2). By increasing the negative DEP forces, PBMCs are pushed further away from the chamber floor resulting in fewer PBMCs being collected in the collection port. However, because cancer cell levitation is minimized by precise control of injection and eluate flow rates, increasing the applied voltage has minimal impact on cancer cell collection as cancer cells already flow close to the chamber floor over the electrode for collection. The DOE analysis showed that in the operating ranges tested, frequency was the critical factor for cancer cell collection and voltage was the critical factor for PBMC contamination. Furthermore, our analysis has demonstrated that the increase in the collection flow rate resulted in higher cancer cell recovery, probably due to an increase in the skimming height (data not shown). However, higher collection flow rates also resulted in an increase in PBMC contamination.

To demonstrate response to frequency and sample injection flow rate, a DOE was executed and results were analyzed using RSM. Cancer cell recovery increased with an increase in frequency from 45 kHz to 65 kHz (Figure 3(a)). Indeed, the mean crossover frequency of SKOV3 cancer cells was shown to be about 40 kHz, suggesting that increasing frequency above 40 kHz would have resulted in stronger positive DEP forces and augmented collection efficiency. There was no statistically significant change in PBMC reduction over the 45 kHz to 65 kHz frequency
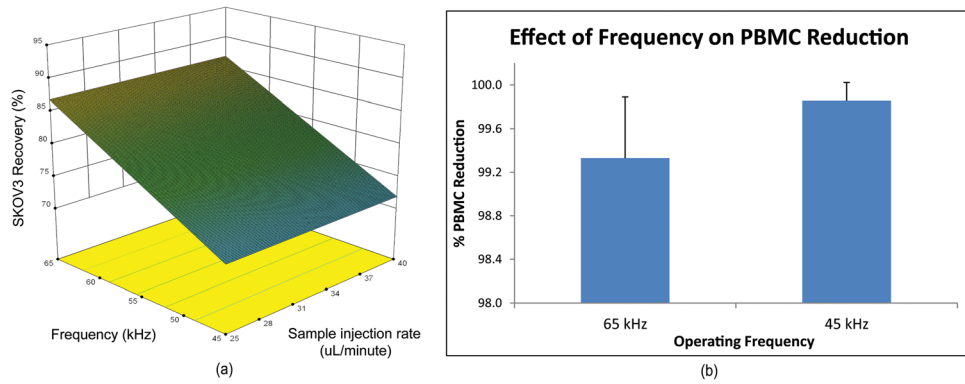
FIG. 3. (a) RSM plot for the ApoStream flow chamber showing cancer cell recovery response to frequency and sample injection flow rate. (b) Effect of operating frequency on percentage PBMC reduction after ApoStream separation.

range tested as these frequencies are well below the average crossover frequencies of PBMCs (Figure 3(b)). The average percentage reduction in PBMCs after ApoStream separation was found to be $99.33\% \pm 0.56\%$ at 65 kHz and $99.85\% \pm 0.17\%$ at 45 kHz operating frequency. There was no significant change in the recovery with an increase in the sample injection rate
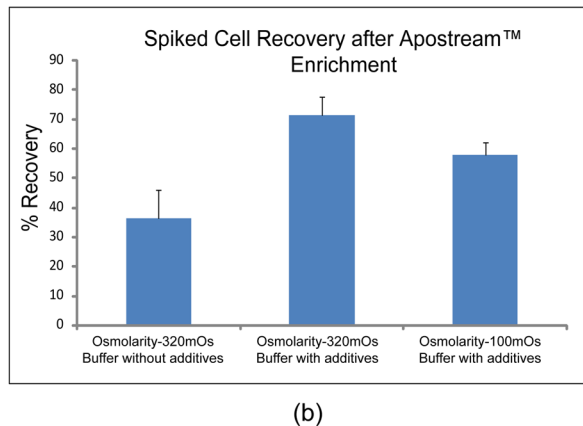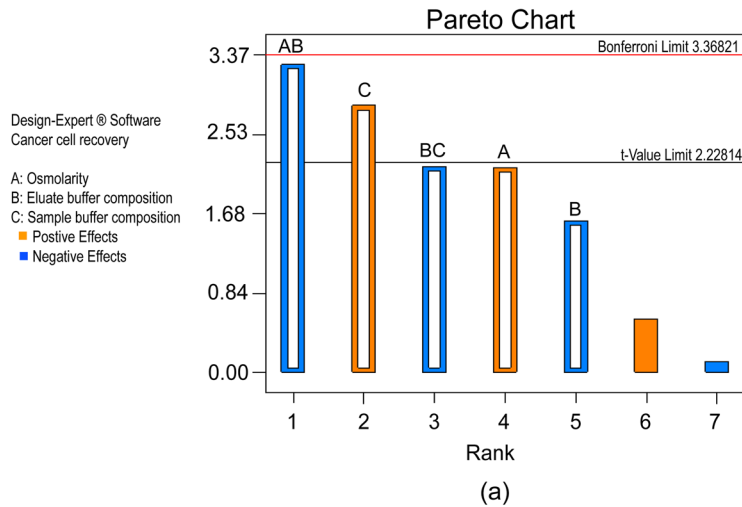
FIG. 4. Buffer optimization for the ApoStream device using SKOV3 cancer cells spiked in PBMCs. (a) Pareto chart from DOE analysis showing sample buffer composition as the only significant factor with a positive effect on cancer cell recovery. (b) Sample buffer with additives improves cancer cell recovery.

within the range tested (Figure 3(a)). Although higher sample injection rates could have resulted in higher cell levitation in the flow chamber, the results from the chosen flow chamber configuration demonstrate sufficient travel time was allowed for cells to settle sufficiently to come within the reach of the DEP field and become attracted towards the electrode surface.

C. Buffer optimization

Eluate and sample buffer optimization studies were performed to further maximize cancer cell recovery. Statistical analysis of the results indicated that the sample buffer composition was the only significant factor with a positive effect on cancer cell recovery as shown in the Pareto chart (above t-value limit) (Figure 4(a)). Cancer cell recovery improved when using sample buffer with additives compared to no additives or at lower osmolarity eluate buffer (Figure 4(b)). Buffer additives such as BSA, pluronic F-68, anti-oxidant compound, and catalase are known to provide either cell membrane stability, reduction of oxidative stress, or decreased aggregation.[48,49] BSA has been known to reduce the non-specific cell surface interactions and is widely used in flow cytometry and microfluidic applications.[49] Pluronic F-68 is a stabilizer of cell membranes; it reduces potential for membrane shearing by enhancing mechanical strength of the cell membrane with short-term exposure.[50] It has been shown that hydrogen peroxide is produced when sugar-containing buffer is exposed to AC electric fields; the addition of catalase to buffer allows hydrogen peroxide decomposition and reduces potential for cell damage.[48] These additives were used in the sample buffer to improve the device performance based on their known beneficial effects on cells and ability to increase recovery by lowering non-specific adhesion between cell to cell and cell to contact surfaces.

TABLE I. Intra-day and inter-day precision of the ApoStream device for the recovery of approximately 5000 SKOV3 and 500 MDA-MB-231 cells spiked into PBMCs from 7.5 ml of normal human donor blood.

	Day of run	Replicate	% Cancer cell recovery	Average % cancer cell recovery	Standard deviation	Coefficient of variation (%CV)
Intra-day precision (SKOV3 cells)	Day 1	Sample 1	75.0	74.9	2.0	2.7
		Sample 2	73.8			
		Sample 3	77.6			
		Sample 4	73.1			
Inter-day precision (SKOV3 cells)	Day 1	Sample 1	77.4	76.2		
		Sample 2	71.0			
		Sample 3	78.7			
		Sample 4	77.5			
	Day 2	Sample 5	75.0	74.9	0.7	0.9
		Sample 6	73.8			
		Sample 7	77.6			
		Sample 8	73.1			
	Day 3	Sample 9	81.4	75.2		
		Sample 10	75.2			
		Sample 11	72.7			
		Sample 12	71.6			
Intra-day precision (MDA-MB-231 cells)	Day 1	Sample 1	69.1	70.0	0.9	1.2
		Sample 2	70.8			
		Sample 3	70.0			
Inter-day precision (MDA-MB-231 cells)	Day 1	Sample 1	73.4	72.4	1.1	1.5
	Day 2	Sample 2	72.6			
	Day 3	Sample 3	71.2			
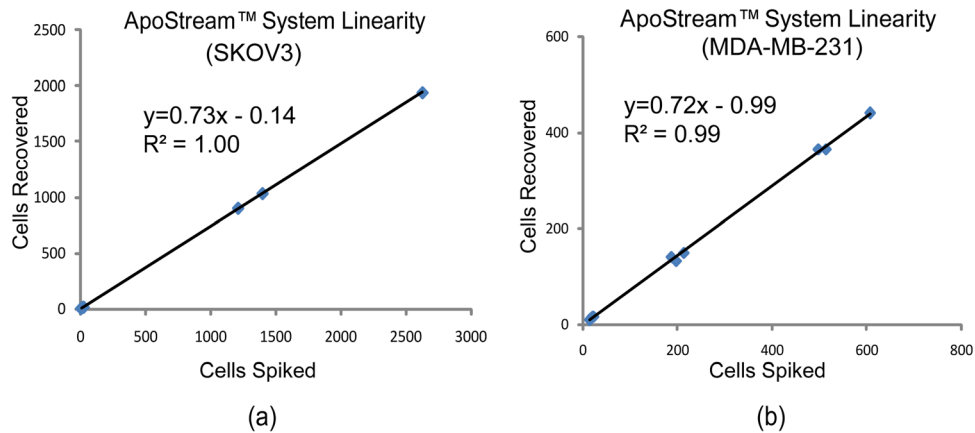
FIG. 5. ApoStream device linearity for (a) SKOV3 and (b) MDA-MB-231 spiked cell recovery.

D. Device performance and characterization

Cancer cell recovery performance was assessed via systematic precision and linearity spiking studies with 2 different cancer cell lines. The intra-day and inter-day precision results for the enrichment of SKOV3 and MDA-MB-231 cells are shown in Table I. The overall average recovery of tumor cells spiked into approximately 12×10^6 PBMCs (isolated from 7.5 ml normal human donor blood) was $75.4\% \pm 3.1\%$ (n = 12) and $71.2\% \pm 1.6\%$ (n = 6) for SKOV3 and MDA-MB-231 cells, respectively. Both the intra-day and inter-day precision of the device were less than 3% CV and inter-system CV% was 0.1% (data not shown). The recovery efficiencies are comparable to other DEP-based devices for cancer cell isolation. The efficiency of ovarian cancer cell enrichment was 76% using circular microelectrodes.[24] The recovery efficiency of MCF-7 breast cancer cell line from normal breast cells was found to be maximum at 86.6% using dielectrophoresis-activated cell sorter.[29] The separation efficiency of MCF-7 cells from red blood cells (RBCs) and PBMCs was reported as 75.18% using multi-orifice flow fractionation and DEP.[28] Most of these DEP microfluidic chip based devices have lower cell throughput compared to ApoStream.

Device linearity was demonstrated by spiking 4 to ~2600 SKOV3 cells and 14 to ~600 MDA-MB-231 cells into ~12×10^6 PBMCs obtained from 7.5 ml normal human donor blood (Figure 5). The regression equations for linearity were $y = 0.74 \times -0.14$ with a correlation coefficient (R^2) of 1.00 and $y = 0.72 \times -0.99$ with R^2 of 0.99 for SKOV3 and MDA-MB-231 cells, respectively. The recovery performance of the device at lower spiking levels was demonstrated by spiking low numbers of cancer cells into PBMCs and capturing cells with the ApoStream

TABLE II. Cancer cell recovery from ApoStream device for low number of cancer cells spiked into PBMCs from 7.5 ml of normal human donor blood.

	Number of spiked cancer cells	Cancer cells collected after ApoStream™	% Cancer cell recovery	Average % cancer cell recovery
SKOV3 cells	23	14	60.9	
	19	14	73.7	
	5	4	80.0	
	4	2	50.0	68.3
MDA-MB-231 cells	22	16	72.7	
	21	16	76.2	
	14	9	64.3	

system. The average cancer cell recovery at the lower spiking levels ranging from 4 to 23 cells was 68.3% ± 10.4% as shown in Table II. The ApoStream system was able to enrich and collect 2 cancer cells from as few as 4 cells spiked into PBMCs from 7.5 ml of normal donor blood. The recovery precision and linearity data of the ApoStream device demonstrate consistent cancer cell recovery performance for both high and low-EpCAM expressing cancer cell types over a wide range of spiking levels.

The reduction in PBMCs after ApoStream separation was also analyzed. The average percentage reduction in PBMCs after ApoStream separation in the linearity and precision studies reported above was 99.33% ± 0.56% (n = 41). These results compare favorably to other studies. The enrichment factor was found to be only 16 fold for the separation of colorectal cancer cells using DEP microfluidic chip.[22] Another DEP based study showed white blood cell separation
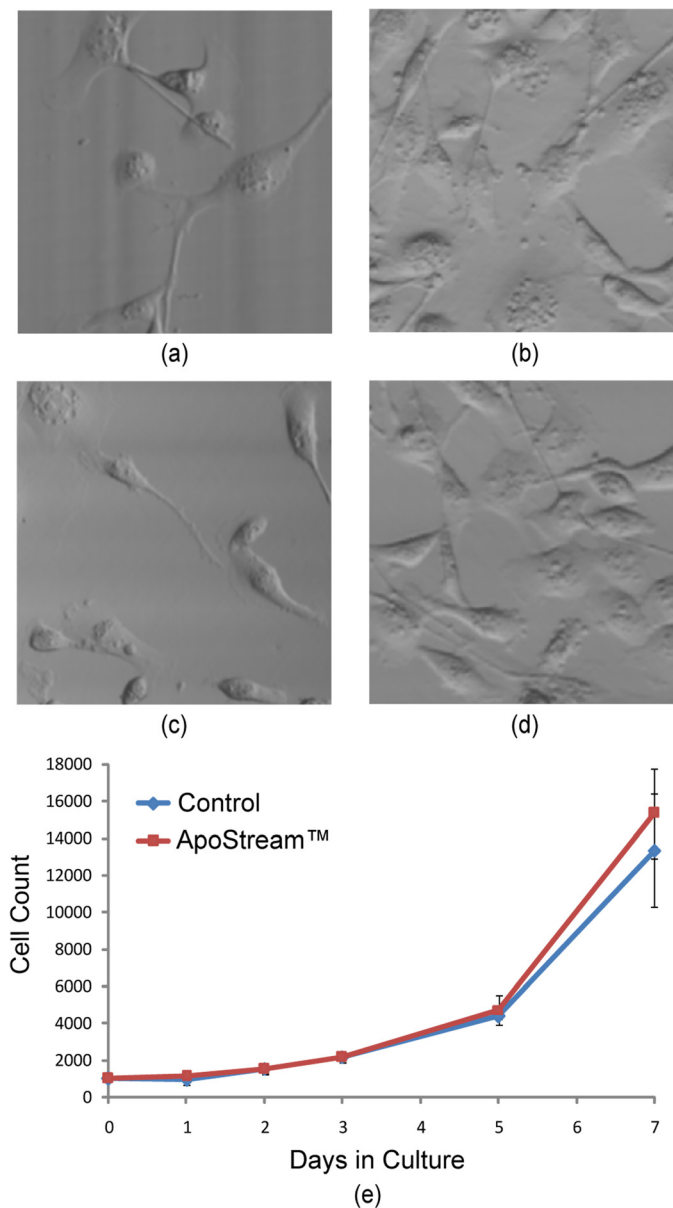
FIG. 6. Images of cultured MDA-MB-231 cancer cells at day 2 and day 7: (a) and (b) control cells (no ApoStream separation); (c) and (d) cells captured with ApoStream; (e) ApoStream recovered MDA-MB-231 cancer cells show exponential growth and no difference compared to control cells (no ApoStream separation).

efficiency of only 94.23% for the isolation of breast cancer cells.[28] To demonstrate capability of achieving higher levels of purity with the ApoStream device, additional testing was performed by processing samples through the ApoStream device twice (double enrichment). After the first separation run, the collected sample was centrifuged at 1000 g for 5 min and resuspended in the sample buffer. The sample was then processed through the ApoStream device a second time. After double enrichment, the average cancer cell recovery was reduced to a cumulative 52% but the percentage reduction in PBMCs increased to as high as 99.99%. The data demonstrated that the PBMC contamination can be reduced significantly through double enrichment of the sample. In addition, the ApoStream device provides flexibility by allowing the user to adjust operating parameters to tailor performance to either maximize recovery or maximize purity. For example, by applying a lower operating frequency (further away from mean crossover frequencies of PBMCs) and lower collection flow rates, performance can be adjusted to reduce the PBMC contamination even further.

E. Cell viability and culture after isolation using ApoStream

Following isolation and enrichment using the ApoStream device, MDA-MB-231 cancer cells were cultured and propagated according to standard tissue culture methods (Figure 6). Trypan blue exclusion measurements indicated that cell viability was not affected by the ApoStream device; cell viability was 97.6% following ApoStream separation and was maintained at >97% during the 7 day culture period. Cells showed normal attachment and spreading over the culture plate at day 2 (Figure 6(c)) and day 7 (Figure 6(d)) after ApoStream separation and were comparable to the controls (Figures 6(a) and 6(b)). Comparable exponential growth was observed (Figure 6(e)) for ApoStream isolated cells and control cells (no ApoStream isolation). These results are consistent with previous findings indicating that exposure to low frequency electric fields does not cause cell damage.[51]

V. CONCLUSION

We have designed and developed a continuous flow dielectrophoretic device for antibody independent, high throughput isolation and recovery of viable cancer cells from blood. Performance characterization of the ApoStream device demonstrated precision and linearity in the recovery of both high and low EpCAM-expressing cancer cells. ApoStream has the potential to isolate and recover viable cancer cells from all cancer types and enables molecular analysis of the cancer cells. The isolation and recovery of cancer cells from blood using ApoStream represent a significant advancement in the field of CTCs enrichment and has been incorporated into numerous ongoing clinical trial studies.

ACKNOWLEDGMENTS

[1] I. J. Fidler, Nat. Rev. Cancer **3**, 453 (2003).
[2] K. Pantel and S. Riethdorf, Nat. Rev. Clin. Oncol. **6**, 190 (2009).
[3] W. J. Allard, J. Matera, M. C. Miller, M. Repollet, M. C. Connelly, C. Rao, A. G. Tibbe, J. W. Uhr, and L. W. Terstappen, Clin. Cancer Res. **10**, 6897 (2004).

[4]G. T. Budd, M. Cristofanilli, M. J. Ellis, A. Stopeck, E. Borden, M. C. Miller, J. Matera, M. Repollet, G. V. Doyle, L. W. Terstappen, and D. F. Hayes, Clin. Cancer Res. **12**, 6403 (2006).

[5]J. S. de Bono, H. I. Scher, R. B. Montgomery, C. Parker, M. C. Miller, H. Tissing, G. V. Doyle, L. W. Terstappen, K. J. Pienta, and D. Raghavan, Clin. Cancer Res. **14**, 6302 (2008).

[6]S. J. Cohen, C. J. Punt, N. Iannotti, B. H. Saidman, K. D. Sabbath, N. Y. Gabrail, J. Picus, M. Morse, E. Mitchell, M. C. Miller, G. V. Doyle, H. Tissing, L. W. Terstappen and N. J. Meropol, J. Clin. Oncol. **26**, 3213 (2008).

[7]S. Maheswaran, L. V. Sequist, S. Nagrath, L. Ulkus, B. Brannigan, C. V. Collura, E. Inserra, S. Diederichs, A. J. Iafrate, D. W. Bell, S. Digumarthy, A. Muzikansky, D. Irimia, J. Settleman, R. G. Tompkins, T. J. Lynch, M. Toner, and D. A. Haber, N. Engl. J. Med. **359**, 366 (2008).

[8]M. Cristofanilli, G. T. Budd, M. J. Ellis, A. Stopeck, J. Matera, M. C. Miller, J. M. Reuben, G. V. Doyle, W. J. Allard, L. W. Terstappen, and D. F. Hayes, N. Engl. J. Med. **351**, 781 (2004).

[9]K. Pachmann, O. Camara, A. Kavallaris, S. Krauspe, N. Malarski, M. Gajda, T. Kroll, C. Jorke, U. Hammer, A. Altendorf-Hofmann, C. Rabenstein, U. Pachmann, I. Runnebaum, and K. Hoffken, J. Clin. Oncol. **26**, 1208 (2008).

[10]L. M. Flores, D. W. Kindelberger, A. H. Ligon, M. Capelletti, M. Fiorentino, M. Loda, E. S. Cibas, P. A. Janne, and I. E. Krop, Br. J. Cancer **102**, 1495 (2010).

[11]I. Desitter, B. S. Guerrouahen, N. Benali-Furet, J. Wechsler, P. A. Janne, Y. Kuang, M. Yanagita, L. Wang, J. A. Berkowitz, R. J. Distel, and Y. E. Cayre, Anticancer Res. **31**, 427 (2011).

[12]G. Vona, A. Sabile, M. Louha, V. Sitruk, S. Romana, K. Schutze, F. Capron, D. Franco, M. Pazzagli, M. Vekemans, B. Lacour, C. Brechot, and P. Paterlini-Brechot, Am. J. Pathol. **156**, 57 (2000).

[13]S. Nagrath, L. V. Sequist, S. Maheswaran, D. W. Bell, D. Irimia, L. Ulkus, M. R. Smith, E. L. Kwak, S. Digumarthy, A. Muzikansky, P. Ryan, U. J. Balis, R. G. Tompkins, D. A. Haber, and M. Toner, Nature **450**, 1235 (2007).

[14]S. L. Stott, C. H. Hsu, D. I. Tsukrov, M. Yu, D. T. Miyamoto, B. A. Waltman, S. M. Rothenberg, A. M. Shah, M. E. Smas, G. K. Korir, F. P. Floyd, Jr., A. J. Gilman, J. B. Lord, D. Winokur, S. Springer, D. Irimia, S. Nagrath, L. V. Sequist, R. J. Lee, K. J. Isselbacher, S. Maheswaran, D. A. Haber, and M. Toner, Proc. Natl. Acad. Sci. U.S.A. **107**, 18392 (2010).

[15]X. Zhe, M. L. Cher, and R. D. Bonfil, Am. J. Cancer Res. **1**, 740 (2011).

[16]P. Helo, A. M. Cronin, D. C. Danila, S. Wenske, R. Gonzalez-Espinoza, A. Anand, M. Koscuiszka, R. M. Vaananen, K. Pettersson, F. K. Chun, T. Steuber, H. Huland, B. D. Guillonneau, J. A. Eastham, P. T. Scardino, M. Fleisher, H. I. Scher, and H. Lilja, Clin. Chem. **55**, 765 (2009).

[17]G. Spizzo, D. Fong, M. Wurm, C. Ensinger, P. Obrist, C. Hofer, G. Mazzoleni, G. Gastl and P. Went, J. Clin. Pathol. **64**, 415 (2011).

[18]P. T. Went, A. Lugli, S. Meier, M. Bundi, M. Mirlacher, G. Sauter, and S. Dirnhofer, Hum. Pathol. **35**, 122 (2004).

[19]P. R. Gascoyne, J. Noshari, T. J. Anderson, and F. F. Becker, Electrophoresis **30**, 1388 (2009).

[20]S. Shim, P. Gascoyne, J. Noshari, and K. S. Hale, Integr. Biol. (Camb) **3**, 850 (2011).

[21]R. Pethig, Biomicrofluidics **4**, 022811 (2010).

[22]F. Yang, X. Yang, H. Jiang, P. Bulkhaults, P. Wood, W. Hrushesky, and G. Wang, Biomicrofluidics **4**, 13204 (2010).

[23]A. Salmanzadeh, H. Kittur, M. B. Sano, P. C. Roberts, E. M. Schmelz, and R. V. Davalos, Biomicrofluidics **6**, 24104 (2012).

[24]C. P. Jen and H. H. Chang, Biomicrofluidics **5**, 34101 (2011).

[25]L. Altomare, M. Borgatti, G. Medoro, N. Manaresi, M. Tartagni, R. Guerrieri, and R. Gambari, Biotechnol. Bioeng. **82**, 474 (2003).

[26]L. M. Broche, N. Bhadal, M. P. Lewis, S. Porter, M. P. Hughes, and F. H. Labeed, Oral Oncol. **43**, 199 (2007).

[27]A. C. Sabuncu, J. A. Liu, S. J. Beebe, and A. Beskok, Biomicrofluidics **4**, 021101 (2010).

[28]H. S. Moon, K. Kwon, S. I. Kim, H. Han, J. Sohn, S. Lee, and H. I. Jung, Lab Chip **11**, 1118 (2011).

[29]J. An, J. Lee, S. H. Lee, J. Park, and B. Kim, Anal Bioanal. Chem. **394**, 801 (2009).

[30]Y. Kang, D. Li, S. A. Kalams, and J. E. Eid, Biomed. Microdevices **10**, 243 (2008).

[31]P. Gascoyne, C. Mahidol, M. Ruchirawat, J. Satayavivad, P. Watcharasit, and F. F. Becker, Lab Chip **2**, 70 (2002).

[32]I. F. Cheng, H. C. Chang, D. Hou, and H. C. Chang, Biomicrofluidics **1**, 21503 (2007).

[33]F. H. Labeed, H. M. Coley, and M. P. Hughes, Biochim. Biophys. Acta **1760**, 922 (2006).

[34]E. G. Cen, C. Dalton, Y. Li, S. Adamia, L. M. Pilarski, and K. V. Kaler, J. Microbiol. Methods **58**, 387 (2004).

[35]X. B. Wang, J. Yang, Y. Huang, J. Vykoukal, F. F. Becker, and P. R. Gascoyne, Anal. Chem. **72**, 832 (2000).

[36]Y. Huang, X. B. Wang, F. F. Becker, and P. R. Gascoyne, Biophys J. **73**, 1118 (1997).

[37]H. Markx, J. Rousselet, and R. Pethig, J. Liq. Chrom. Rel. Technol. **20**, 2857 (1997).

[38]J. Rousselet, G. H. Markx, and R. Pethig, Colloids Surf. A **140**, 209 (1998).

[39]M. Abraham, *The Classical Theory of Electricity and Magnetism* (Hafner, New York, 1932).

[40]T. B. Jones, *Electromechanics of Particles* (Cambridge University Press, Cambridge, 1995).

[41]Y. J. Lo and U. Lei, Appl. Phys. Lett. **95**, 253701 (2009).

[42]G. H. Markx, R. Pethig, and J. Rousselet, J. Phys. D: Appl. Phys. **30**, 2470 (1997).

[43]X. B. Wang, Y. Huang, J. P. H. Burt, G. H. Markx, and R. Pethig, J. Phys. D: Appl. Phys. **26**, 1278 (1993).

[44]G. H. Markx and R. Pethig, Biotechnol. Bioeng. **45**, 337 (1995).

[45]R. S. Kuczenski, H. C. Chang, and A. Revzin, Biomicrofluidics **5**, 32005 (2011).

[46]X. Hu, P. H. Bessette, J. Qian, C. D. Meinhart, P. S. Daugherty, and H. T. Soh, Proc. Natl. Acad. Sci. U.S.A. **102**, 15757 (2005).

[47]M. P. Hughes, R. Pethig, and X. B. Wang, J. Phys. D: Appl. Phys. **29**, 474 (1996).

[48]X. Wang, J. Yang, and P. R. Gascoyne, Biochim. Biophys. Acta **1426**, 53 (1999).

[49]G. L. Francis, Cytotechnology **62**, 1 (2010).

[50]Z. Zhang, M. Al-Rubeai, and C. R. Thomas, Enzyme Microb. Technol. **14**, 980 (1992).

[51]R. Pethig and G. H. Markx, Trends Biotechnol. **15**, 426 (1997).